Journal of Molecular Liquids 215 (2016) 740–748

Contents lists available at ScienceDirect

Journal of Molecular Liquids

journal homepage: www.elsevier.com/locate/molliq

Molecular docking, potentiometric and thermodynamic studies of some azo quinoline compounds

A.F. Shoair *, A.A. El-Bindary, A.Z. El-Sonbati, N.M. Beshry

Chemistry Department, Faculty of Science, Damietta University, Damietta 34517, Egypt

ARTICLE INFO

Article history:
Received 22 October 2015
Received in revised form 18 December 2015
Accepted 23 December 2015
Available online xxxx

Keywords:
Quinoline azodye
Potentiometry
Thermodynamic parameters
Molecular docking
X-ray diffraction

ABSTRACT

The ligands of 5-(4-derivative phenyl azo)-8-hydroxyquinoline and its derivatives ($\mathbf{HL_n}$) were synthesized from the coupling of the quinoline with diazonium salt derived from aniline and its *p*-derivatives and characterized by different spectroscopic techniques. Molecular docking was used to predict the binding between azo compounds with the receptor of breast cancer mutant 3hb5-oxidoreductase. The X-ray diffraction, XRD, pattern of the ligand ($\mathbf{HL_3}$) is polycrystalline nature. The proton-ligand dissociation constant of the azo compounds ($\mathbf{HL_n}$) and metal–ligand stability constants of their complexes with metal ions (Mn^{2+}, Co^{2+}, Ni^{2+} and Cu^{2+}) have been determined by potentiometric technique in 0.1 M KCl and 50% (by volume) DMF–water mixture. For the same ligand at constant temperature, the stability constants of the formed complexes increase in the order Mn^{2+}, Co^{2+}, Ni^{2+} and Cu^{2+}. The effect of temperature was studied at 298, 308 and 318 K and the corresponding thermodynamic parameters (ΔG, ΔH and ΔS) were derived and discussed. The dissociation process is non-spontaneous, endothermic and entropically unfavorable. The formation of the metal complexes has been found to be spontaneous, endothermic and entropically favorable.

1. Introduction

Quinoline azodye and its derivatives are very important compounds and have attracted much attention in both academic and applied research used in many applications such as their biological relevance, coordination capacity, their use as metal extracting agent and their therapeutic properties [1–6]. Also the azo compounds based on quinoline play a central role as chelating agents for a large number of metal ions, as they form a stable six and/or five-membered ring after complexation with the metal ion [4,6]. The azo compounds are used in dying processes; some of them are used in analytical separation of many metal ions in a mixture. It is well-known that N atoms play a key role in the coordination of metals at the active sites of numerous metallobiomolecules [7].

The potentiometric study is one of the most convenient and successful technique employed for metal complex equilibrium measurements. Such applications are based on studying the influence of the pH on the equilibrium system components; metal ion, ligand and proton [8,9]. The use of protein–ligand docking has become a standard method in potentiometric studies [10]. The protein groups surrounding the ligand can highly influence the local pH, so that a different protonation could be favored in the bound state. The molecular docking is widely used to predict protein–ligand [10,11] and to screen large libraries for molecules that will modulate the activity of a biological receptor.

In this paper, the potentiometric studies are used to determine the dissociation constants of 5-(4-derivative phenyl azo)-8-hydroxyquinoline ($\mathbf{HL_n}$) and the stability constants of its complexes with some divalent transition metal ions such as Mn^{2+}, Co^{2+}, Ni^{2+} and Cu^{2+} at different temperatures. The corresponding thermodynamic functions are evaluated and discussed. Moreover, the molecular docking of the ligands ($\mathbf{HL_n}$) is studied.

2. Materials and methods

All the compounds and solvents used were purchased from Aldrich and Sigma and used as received without further purification.

2.1. Preparation of the ligands

The ligands of 5-(4-derivative phenyl azo)-8-hydroxyquinoline and its derivatives ($\mathbf{HL_n}$) were prepared by dissolving aniline or its *p*-substituted derivatives (10 mmol) in hydrochloric acid [12,13]. The compound was diazotized below −5 °C in an ice–salt bath with a solution of sodium nitrite (0.8 g, 10 mmol, 30 ml distilled H_2O). The diazonium salt was coupled with an alkaline solution of quinoline-8-ol (1.0 g, 10 mmol) in pyridine. The precipitate was filtered and dried after thorough washing with water and ethanol. The crude products were purified by recrystallization from hot ethanol and dried in vacuum

* Corresponding author.
E-mail address: abdel_shoair@yahoo.com (A.F. Shoair).

http://dx.doi.org/10.1016/j.molliq.2015.12.081
0167-7322/

desiccator over P_2O_5. Yield percent was 65–81%. The ligands are also characterized by IR and ^1H NMR spectroscopies (Fig. 1).

HL_1 = 5-(4-methoxyphenyl azo)-8-hydroxyquinoline.
HL_2 = 5-(4-methylphenyl azo)-8-hydroxyquinoline.
HL_3 = 5-(phenyl azo)-8-hydroxyquinoline.
HL_4 = 5-(4-chlorophenyl azo)-8-hydroxyquinoline.

2.2. Potentiometric studies

A ligand solution (0.001 M) was prepared by dissolving an accurately weighted amount of the solid in DMF. Metal ion solutions (0.0001 M) were prepared from metal chlorides in bidistilled water and standardized with EDTA [14]. Solutions of 0.001 M HCl and 1 M KCl were also prepared in bidistilled water. A carbonate-free NaOH solution in 50% (by volume) DMF–water mixture was used as titrant and standardized against oxalic acid.

The apparatus, general conditions and methods of calculation were the same as in previous work [15,16]. The following mixtures (i)–(iii) were prepared and titrated potentiometrically at 298 K against standard 0.002 M NaOH in a 50% (by volume) DMF–water mixture:

i) 5 cm^3 0.001 M HCl + 5 cm^3 1 M KCl + 25 cm^3 DMF.
ii) 5 cm^3 0.001 M HCl + 5 cm^3 1 M KCl + 20 cm^3 DMF + 5 cm^3 0.001 M ligand.
iii) 5 cm^3 0.001 M HCl + 5 cm^3 l M KCl + 20 cm^3 DMF + 5 cm^3 0.001 M ligand + 10 cm^3 0.0001 M metal chloride.

For each mixture, the volume was made up to 50 cm^3 with bidistilled water before the titration. These titrations were repeated for the temperatures of 308 and 318 K. All titrations have been carried out between pH 3.5 and 13.0 and under nitrogen atmosphere.

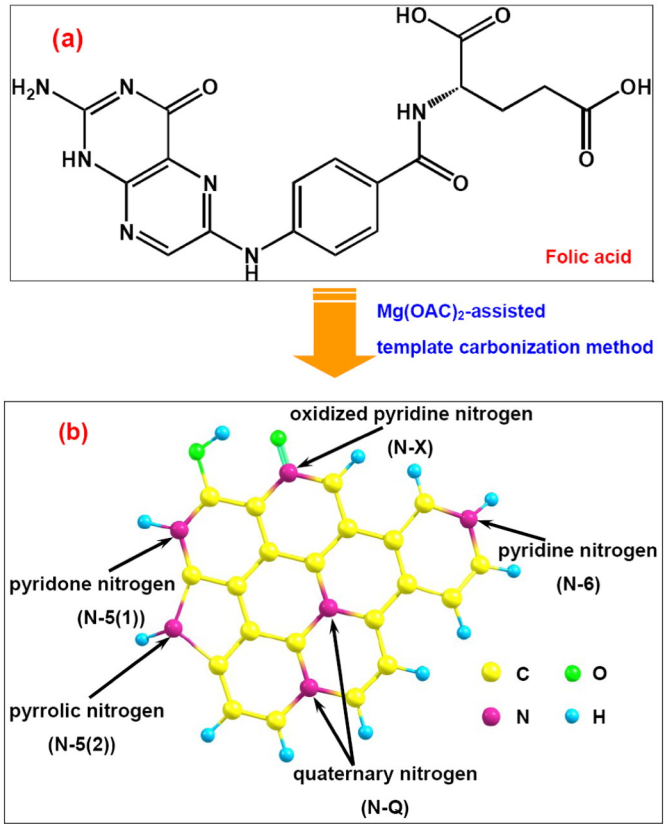

Fig. 1. The formation mechanism of azo quinoline derivatives (HL_n).

Table 1
Analytical data of the ligands ($\mathbf{HL_n}$).

Compound	Exp. (Calc.) %		
	C	H	N
$\mathbf{HL_1}$	68.64 (68.82)	4.52 (4.66)	14.84 (15.05)
$\mathbf{HL_2}$	72.87 (73.00)	4.78 (4.94)	15.67 (15.97)
$\mathbf{HL_3}$	72.12 (72.29)	4.20 (4.42)	16.51 (16.87)
$\mathbf{HL_4}$	63.26 (63.49)	3.32 (3.53)	14.44 (14.82)

2.3. Measurements

Elemental microanalyses of the separated ligands for C, H and N were determined on Automatic Analyzer CHNS Vario ELIII, Germany. FT-IR spectra (KBr disks, 4000–400 cm^{-1}) by Jasco-4100 spectrophotometer. The ^1H NMR spectra by Bruker WP 300 MHz using DMSO-d_6 as a solvent containing TMS as the internal standard. X-ray diffraction measurement (XRD) is recorded on X-ray diffractometer in the range of diffraction angle $2\theta^o$ = 5–80°. This analysis is carried out using $CuK_{\alpha 1}$ radiation (λ = 1.540598 Å). The applied voltage and the tube current are 40 KV and 30 mA, respectively. The pH measurements were performed with a Metrohm 836 Titrando (KF & Potentiometric Titrator) equipped with a combined porolyte electrode. The temperature was controlled to within ±0.05 K by circulating thermostated water (Neslab 2 RTE 220) through the outer jacket of the vessel.

Docking calculations were carried out using a Docking Server [17–19]. The MMFF94 force field [20] was used for energy minimization of ligand molecule using Docking Server. Gasteiger partial charges were added to the ligand atoms. Non-polar hydrogen atoms were merged and rotatable bonds were defined. Docking calculations were carried out on 3hb5-oxidoreductase protein model. Essential hydrogen atoms, Kollman united atom type charges, and solvation parameters were added with the aid of AutoDock tools [21]. Affinity (grid) maps of 20 × 20 × 20 Å grid points and 0.375 Å spacing were generated using the Autogrid program [21]. AutoDock parameter set- and distance-dependent dielectric functions were used in the calculation of the van der Waals and the electrostatic terms, respectively. Docking simulations were performed using the Lamarckian genetic algorithm (LGA) and the Solis & Wets local search method [22]. Initial position, orientation and torsions of the ligand molecules were set randomly. Each docking experiment was derived from 10 different runs that were set to terminate after a maximum of 250,000 energy evaluations. The population size was set to 150. During the search, a translational step of 0.2 Å, and quaternion and torsion steps of 5 were applied.

3. Results and discussion

3.1. Characterization of the ligands (HL_n)

The chemical structures of the ligands were elucidated by elemental analyses Table 1. The infrared spectra of ligands (HL_n) shows two bands in the range of 3266–3315 and 1570–1590 cm^{-1} for stretching OH of quinoline at C_8-position and $CN_{quin.}$ (nitrogen atom of azomethine of quinoline group), respectively. The aromatic C–H bands was observed at 3000–3120 cm^{-1} as used and methyl C–H vibration of methoxy group was observed at 2990–2850 cm^{-1} and exhibit band in the range of 1500–1504 cm^{-1} which could be assigned to υN═N stretching vibration [23–27].

^1H NMR spectra of ligands (HL_n) were recorded in dimethylsulphoxide (DMSO-d_6) solution using tetramethylsilane (TMS) as internal standard. The ^1H NMR spectra of quinoline and benzene rings appeared in the range of 7.01–8.25 ppm. For the $\mathbf{HL_1}$ has a singlet observed at 3.88 ppm is assigned to OCH_3 protons (the integration curve shows three protons). Also $\mathbf{HL_2}$ has a singlet at 3.76 ppm which is assigned to the CH_3 protons. The ^1H NMR spectra show two

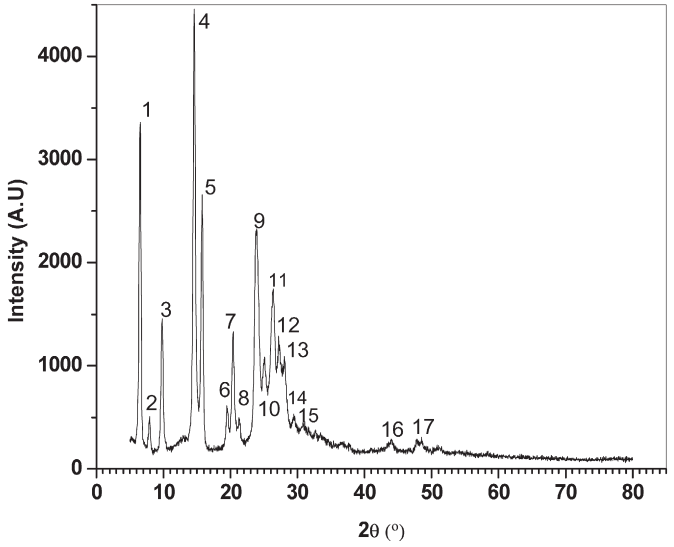

Fig. 2. X-ray diffraction pattern of HL_3 in powder form.

Table 2
Crystallographic data of HL_3.

Peak no.	$2\theta_{obs.}$ (°)	$d_{obs.}$ (Å)	$d_{cal.}$ (Å)	(*h k l*)
1	6.514	13.56162	13.70641	011.
2	7.917	11.16377	11.21252	111.
3	9.788	9.030481	8.988331	$\bar{2}10.$
4	14.586	6.070134	6.070134	$\bar{1}13.$
5	15.772	5.614431	5.606259	222.
6	19.490	4.5526	4.563389	033.
7	20.388	4.354438	4.344614	412.
8	21.288	4.170547	4.170547	323.
9	23.871	3.724855	3.730266	$\bar{4}32.$
10	24.110	3.689176	3.692713	$\bar{2}34.$
11	25.052	3.553044	3.562905	$\bar{5}22.$
12	26.359	3.378509	3.385934	$\bar{3}43.$
13	27.205	3.276478	3.275085	053.
14	28.082	3.175185	3.176495	325.
15	29.584	3.017235	3.0196	344.
16	44.022	2.055778	2.055778	$\bar{7}63.$
17	47.760	1.902915	1.902915	$\bar{5}84.$

singlets for C_8–OH at ~9.55–10.30 ppm and HCN at ~9.09–9.30 ppm [12].

3.2. X-ray diffraction analysis

The X-ray diffraction (XRD) pattern of **HL_3** ligand in powder form is shown in Fig. 2. The XRD pattern shows that the ligand (**HL_3**) has a polycrystalline nature. The calculated crystal system of **HL_3** is found to be monoclinic with space group P21/A. The estimated lattice parameters are found to be 20.4710 Å, 18.8150 Å, 19.9590 Å, 90.0°, 92.7° and 90.0° for a, b, c, α, β and γ, respectively. The inter-planar spacing (*d*) and Miller indices (*hkl*) which are estimated by CRYSFIRE are listed in Table 2.

3.3. Molecular docking

The docking study showed a favorable interaction between the receptor breast cancer (3hb5) and the ligands of 5-(4-derivative phenyl azo)-8-hydroxyquinoline and its derivatives (**HL_n**) and the calculated energy is listed in Table 3 and Fig. 3. According to the results obtained in this study, HB plot curve indicated that, the ligands (**HL_n**) bind to the protein with hydrogen bond interactions and decomposed interaction energies in kcal/mol were existing between the ligands (**HL_n**) with 3hb5 receptor as shown in Fig. 4. The calculated efficiency is favorable where K_i values estimated by AutoDock were compared with experimental K_i values, when available, and the Gibbs free energy is negative. Also, based on this data, we can propose that interaction between the 3hb5 receptor and the ligands (**HL_n**) is possible. 2D plot curves of docking with ligands (**HL_n**) are shown in Fig. 5. This interaction could activate apoptosis in cancer cells energy of interactions with ligands (**HL_n**). Binding energies are most widely used as mode of measuring binding affinity of ligands. Thus, decrease in binding energy due to mutation will increase the binding affinity of the ligands towards the receptor [10]. The characteristic feature of ligands was represented in the presence of several active sites available for hydrogen bonding.

3.4. Potentiometric studies

The hydrogen ion concentration, $[H^+]$, was determined potentiometerically in the usual manner [10]. The average number of the protons associated with ligands (**HL_n**) at different pH values, $\bar{n}_A$, was calculated from the titration curves of the acid in the absence and presence of ligands (**HL_n**) by applying the following equation:

$$\bar{n}_A = Y \pm \frac{(V_1 - V_2)\left(N^0 + E^0\right)}{\left(V^0 - V_1\right)TC_L^0} \quad (1)$$

where Y is the number of available protons in ligands ($Y = 1$) and V_1 and V_2 are the volumes of alkali required to reach the same pH on the titration curve of hydrochloric acid and reagent, respectively, V° is the initial volume (50 cm^3) of the mixture, $TC°_L$ is the total concentration of the reagent, N° is the normality of sodium hydroxide solution and E° is the initial concentration of the free acid. Thus, the formation curves ($\bar{n}_A$ *vs.* pH) for the proton-ligand systems were constructed and found to extend between 0 and 1 in the $\bar{n}_A$ scale. This means that quinoline azo dyes have one ionizable proton (the enolized hydrogen ion of the phenolic –OH group, pK^H as shown in Table 4). The completely protonated form of ligands (**HL_n**) has one dissociable proton, that dissociates in the measurable pH range. The deprotonation of the hydroxyl group most probably results in the formation of stable intramolecular H-bonding with nitrogen of the azo group. Such an interaction decreases the dissociation process of phenolic –OH group, i.e. increases the pK^H value [28,29].

The formation curves for the metal complexes were obtained by plotting the average number of ligands attached per metal ion ($\bar{n}_A$) *vs.*

Table 3
Energy values obtained in docking calculations of ligands (**HL_n**) with receptor breast cancer mutant 3hb5.

Receptor	Est. free energy of binding (kcal/mol)	Est. inhibition constant (K_i) (μM)	vdW + bond + desolve energy (kcal/mol)	Electrostatic energy (kcal/mol)	Total intercooled energy (kcal/mol)	Interact surface
HL_1	−6.23	27.09	−7.64	−0.10	−7.74	732.707
HL_2	−6.83	9.88	−7.67	−0.08	−7.75	710.141
HL_3	−6.72	11.90	−7.64	−0.06	−7.71	659.553
HL_4	−7.46	3.41	−8.14	−0.05	−8.20	716.271

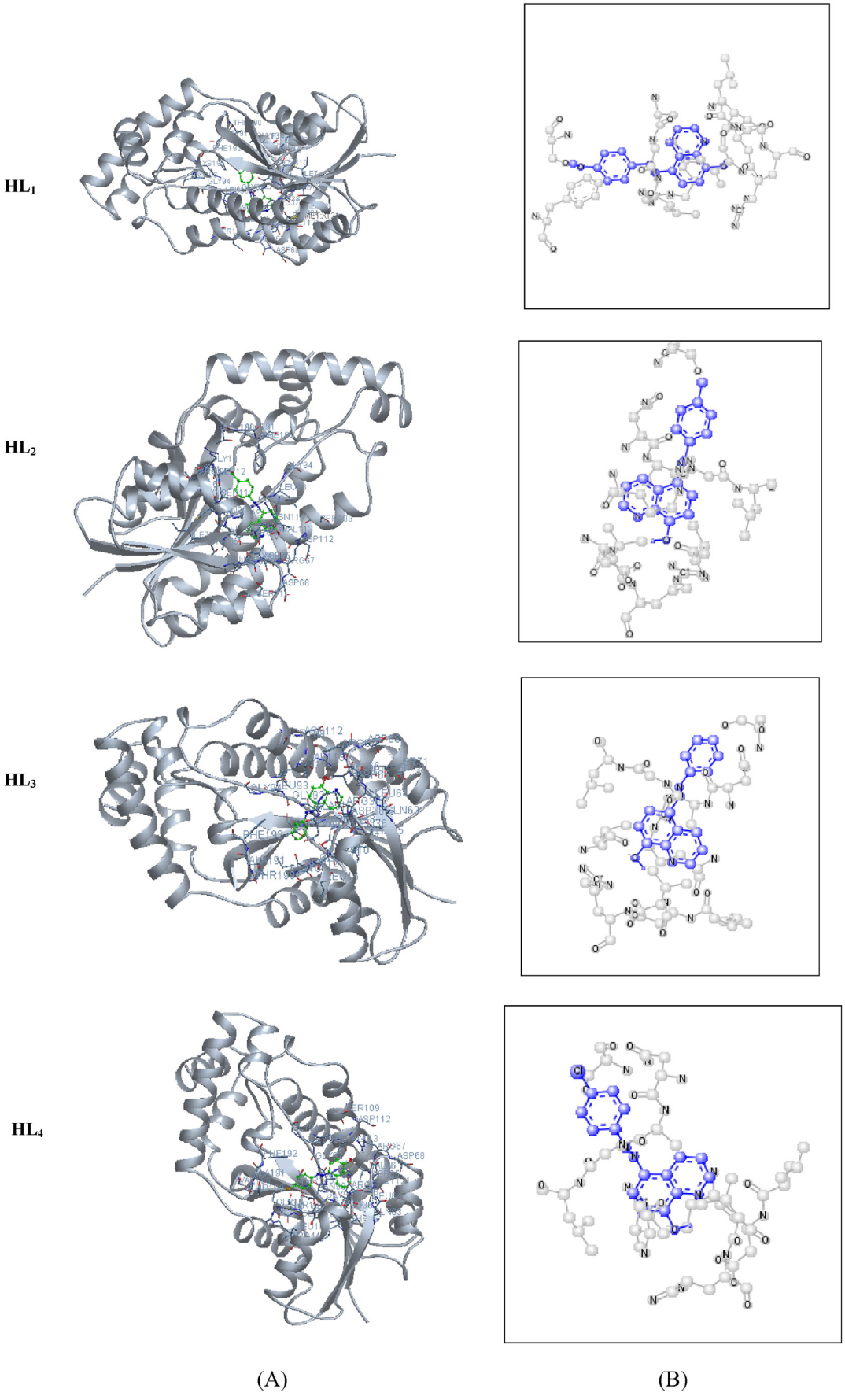

Fig. 3. The ligands (HL_n) (green in (A) and blue in (B)) in interaction with receptor breast cancer mutant 3hb5. (For interpretation of the references to color in this figure legend, the reader is referred to the web version of this article).

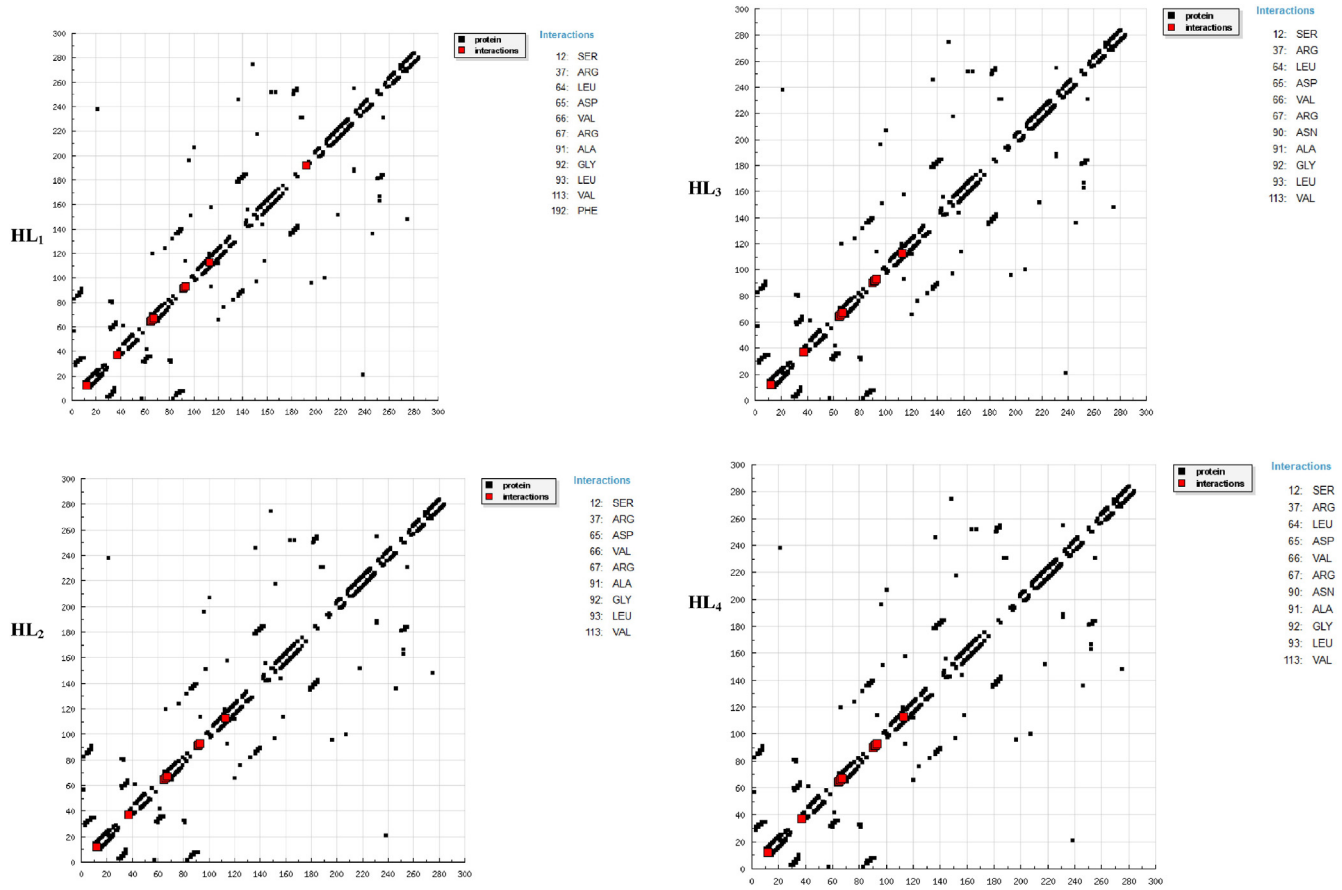

Fig. 4. HB plot of interaction between ligands (HL_n) and receptor breast cancer mutant 3hb5.

the free ligands exponent (pL). The average number of the reagent molecules attached per metal ion, $\bar{n}$, and free ligands exponent, pL, can be calculated using Eqs. (2) and (3):

$$\overline{n}_A = \frac{(V_3 - V_2)(N^{\circ} + E^{\circ})}{(V^{\circ} - V_2)\cdot \overline{n}_A . TC^{\circ}_M} \tag{2}$$

and

$$pL = \log_{10} \frac{\sum_{n=0}^{n=J} \beta_n^H \left(\frac{1}{[H^+]}\right)^n}{TC^0_L - \overline{n}.TC^0_M} \cdot \frac{V^0 + V_3}{V^0} \tag{3}$$

where TC°_M is the total concentration of the metal ion present in the solution, $\beta^H{}_n$ is the overall proton-reagent stability constant. V_1, V_2 and V_3 are the volumes of alkali required to reach the same pH on the titration curves of hydrochloric acid, organic ligand and complex, respectively. These curves were analyzed and the successive metal–ligand stability constants were determined [18]. The values of the stability constants ($\log K_1$ and $\log K_2$) are given in Table 5. The following general remarks can be pointed out:

(i) The maximum value of $\bar{n}$ was ~2 indicating the formation of 1:1 and 1:2 (metal:ligand) complexes only [10].
(ii) The metal ion solution used in the present study was very dilute (2×10^{-5} M), hence there was no possibility of formation of polynuclear complexes [15].
(iii) The metal titration curves were displaced to the right-hand side of the ligand titration curves along the volume axis, indicating proton release upon complex formation of the metal ion with the ligands. The large decrease in pH for the metal titration curves relative to ligand titration curves points to the formation of strong metal complexes [10].
(iv) For the same ligand at constant temperature, the stability of the chelates increases in the order Mn^{2+}, Co^{2+}, Ni^{2+} and Cu^{2+} [16]. This order largely reflects that the stability of Cu^{2+} complexes is considerably larger than those of other metals of the 3d series. Under the influence of both the polarizing ability of the metal ion and the ligands field [10] Cu^{2+} will receive some extra stabilization due to tetragonal distortion of octahedral symmetry in its complexes. The greater stability of Cu^{2+} complexes is produced by the well-known *Jahn–Teller* effect [30].

Stepwise dissociation constants for ligands (**HL_n**) and the stepwise stability constants of their complexes with Mn^{2+}, Co^{2+}, Ni^{2+} and Cu^{2+} have been calculated at 298, 308 and 318 K. The corresponding thermodynamic parameters (ΔG, ΔH and ΔS) were evaluated.

The dissociation constants (pK^H) for ligands (**HL_n**), as well as the stability constants of their complexes with Mn^{2+}, Co^{2+}, Ni^{2+} and Cu^{2+} have been evaluated at 298, 308 and 318 K, and are given in Tables 4 and 5, respectively. The enthalpy (ΔH) for the dissociation and complexation process was calculated from the slope of the plot pK^H or log K *vs.* 1/T as shown in Fig. 6 using the graphical representation of van't Hoff Eqs. (4) and (5):

$$\Delta G = -2.303\, RT \log K = \Delta H - T\Delta S \tag{4}$$

or

$$\log K = \left(\frac{-\Delta H}{2.303R}\right)\left(\frac{1}{T}\right) + \frac{\Delta S}{2.303R} \tag{5}$$

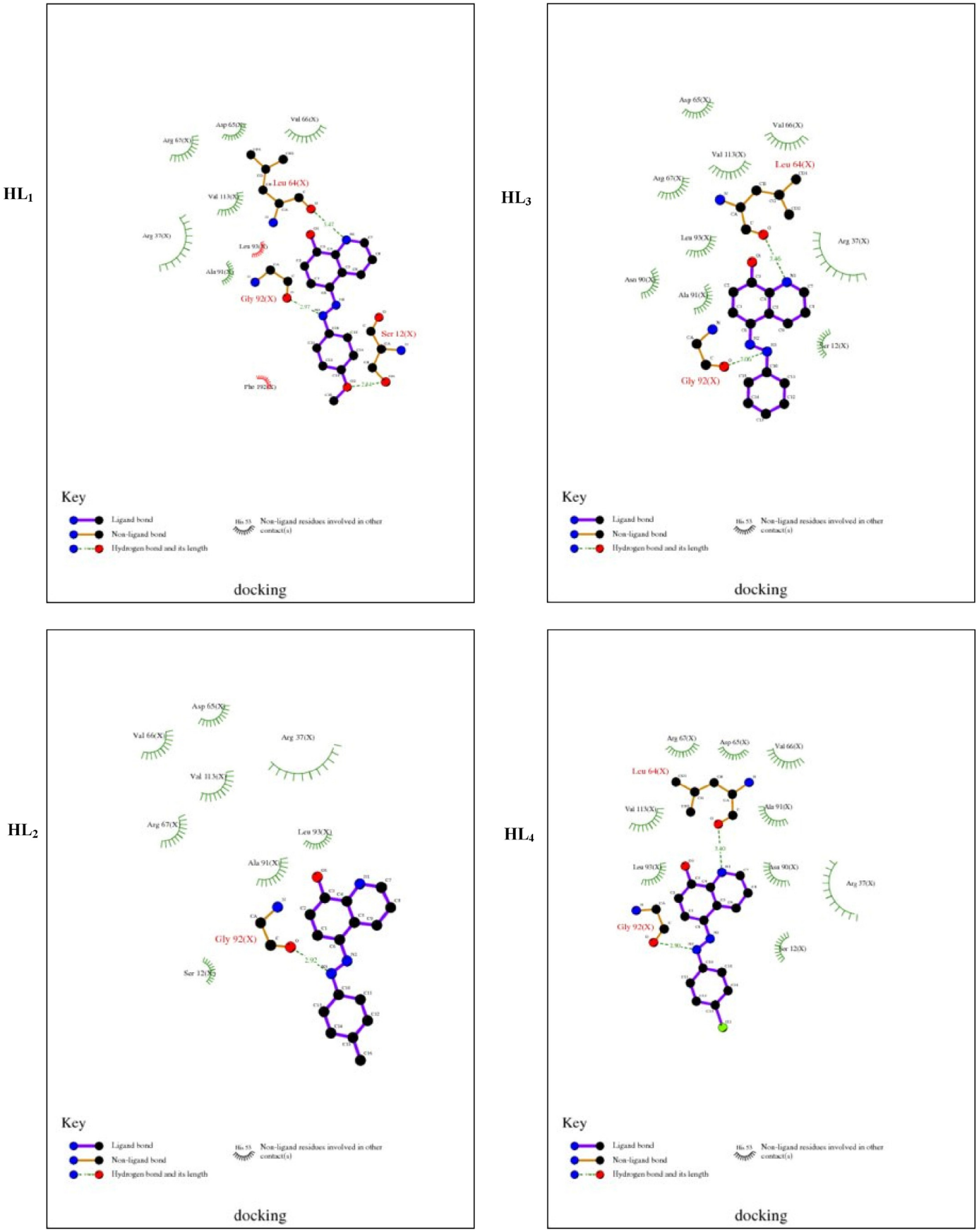

Fig. 5. 2D plot of interaction between ligands (HL_n) and receptor breast cancer mutant 3hb5.

Table 4
Thermodynamic functions for the dissociation of the ligands (**HL_n**) in 50% (by volume) DMF–water mixtures and 0.1 M KCl at different temperatures.

Compound	Temperature (K)	Dissociation constant	Gibbs energy (kJ mol^{-1})	Enthalpy change (kJ mol^{-1})	Entropy change (J mol^{-1} K^{-1})
		pK_1^H	ΔG_1	ΔH_1	$-\Delta S_1$
HL_1	298	9.48	54.09	21.79	108.41
	308	9.35	55.14		108.29
	318	9.24	56.26		108.41
HL_2	298	9.25	52.78	27.21	85.81
	308	9.10	53.67		85.90
	318	8.95	54.49		85.81
HL_3	298	9.00	51.35	26.31	84.03
	308	8.85	52.19		84.03
	318	8.71	53.03		84.04
HL_4	298	8.82	50.33	23.58	89.75
	308	8.69	51.25		89.83
	318	8.56	52.12		89.75

Table 5
Stepwise stability constants for complexes of the ligands (**HL_n**) in 50% (by volume) DMF–water mixtures and 0.1 M KCl at different temperatures.

Comp.	M^{n+}	298 K		308 K		318 K	
		log k_1	log k_2	log k_1	log k_2	log k_1	log k_2
HL_1	Mn^{2+}	5.82	4.59	5.95	4.71	6.09	4.85
	Co^{2+}	5.95	4.64	6.10	4.76	6.22	4.91
	Ni^{2+}	6.10	4.78	6.21	4.90	6.35	5.03
	Cu^{2+}	6.21	4.90	6.35	5.03	6.47	5.15
HL_2	Mn^{2+}	6.00	4.80	6.14	4.93	6.27	5.07
	Co^{2+}	6.12	4.93	6.26	5.05	6.38	5.19
	Ni^{2+}	6.25	5.09	6.40	5.22	6.53	5.35
	Cu^{2+}	6.39	5.22	6.54	5.37	6.68	5.49
HL_3	Mn^{2+}	6.21	4.98	6.35	5.12	6.47	5.24
	Co^{2+}	6.35	5.12	6.49	5.25	6.61	5.40
	Ni^{2+}	6.43	5.26	6.57	5.39	6.70	5.55
	Cu^{2+}	6.55	5.37	6.67	5.50	6.80	5.65
HL_4	Mn^{2+}	6.38	5.16	6.53	5.31	6.67	5.43
	Co^{2+}	6.52	5.30	6.64	5.43	6.78	5.57
	Ni^{2+}	6.66	5.42	6.78	5.55	6.92	5.68
	Cu^{2+}	6.80	5.55	6.92	5.67	7.05	5.79

where R is the gas constant $= 8.314$ J mol^{-1} K^{-1}, K is the dissociation constant for the ligand stability and T is the temperature (K).

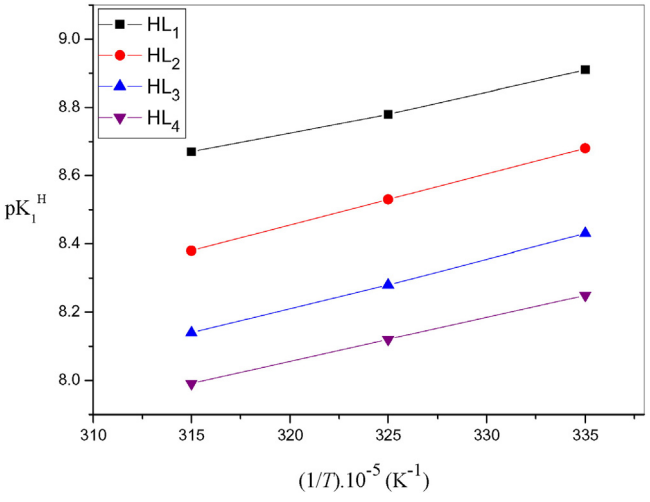

Fig. 6. Van't Hoff plot pK_1^H of ligands (HL_n) against 1/T.

Table 6
Thermodynamic functions for ML and ML_2 complexes of the ligands (**HL_n**) in 50% (by volume) DMF–water mixtures and 0.1 M KCl.

Comp.	M^{n+}	T/K	Gibbs energy (kJ mol^{-1})		Enthalpy change (kJ mol^{-1})		Entropy change (J mol^{-1} K^{-1})	
			$-\Delta G_1$	$-\Delta G_2$	ΔH_1	ΔH_2	ΔS_1	ΔS_2
HL_1	Mn^{2+}	298	26.19	33.21	23.56	24.48	166.95	193.57
		308	27.78	35.09			166.68	193.40
		318	29.53	37.08			166.95	193.58
	Co^{2+}	298	26.48	33.95	24.46	24.52	170.91	196.19
		308	28.07	35.97			170.55	196.40
		318	29.90	37.87			170.92	196.19
	Ni^{2+}	298	27.27	34.81	22.66	22.64	167.57	192.78
		308	28.90	36.62			167.40	192.42
		318	30.63	38.66			167.58	192.79
	Cu^{2+}	298	27.96	35.43	22.68	23.60	169.94	198.10
		308	29.66	37.45			169.95	198.21
		318	31.36	39.39			169.94	198.09
HL_2	Mn^{2+}	298	27.39	34.24	24.48	24.50	174.04	197.09
		308	29.07	36.21			173.87	197.10
		318	30.87	38.18			174.05	197.09
	Co^{2+}	298	28.13	34.92	23.56	23.60	173.46	196.37
		308	29.78	36.92			173.19	196.48
		318	31.60	38.85			173.46	196.37
	Ni^{2+}	298	29.04	35.66	23.58	25.41	176.59	204.95
		308	30.78	37.74			176.51	205.05
		318	32.58	39.76			176.59	204.95
	Cu^{2+}	298	29.78	36.46	24.52	26.31	182.22	210.64
		308	31.67	38.57			182.42	210.65
		318	33.43	40.67			182.21	210.64
HL_3	Mn^{2+}	298	28.42	35.43	23.60	23.60	174.55	198.10
		308	30.19	37.45			174.65	198.21
		318	31.91	39.39			174.54	198.09
	Co^{2+}	298	29.21	36.23	25.37	23.60	183.18	200.78
		308	30.96	38.27			182.91	200.89
		318	32.88	40.25			183.19	200.77
	Ni^{2+}	298	30.01	36.69	26.27	24.50	188.87	205.32
		308	31.79	38.75			188.50	205.33
		318	33.79	40.79			188.88	205.32
	Cu^{2+}	298	30.64	37.37	25.37	22.66	187.97	201.46
		308	32.44	39.34			187.69	201.29
		318	34.40	41.40			187.97	201.47
HL_4	Mn^{2+}	298	29.44	36.40	24.52	26.31	181.07	210.45
		308	31.31	38.51			181.27	210.45
		318	33.06	40.61			181.06	210.45
	Co^{2+}	298	30.24	37.20	24.48	23.56	183.62	203.90
		308	32.02	39.16			183.44	203.63
		318	33.91	41.28			183.62	203.91
	Ni^{2+}	298	30.93	38.00	23.58	23.56	182.90	206.58
		308	32.73	39.98			182.82	206.31
		318	34.58	42.13			182.91	206.59
	Cu^{2+}	298	31.67	38.80	21.77	22.66	179.31	206.25
		308	33.44	40.81			179.23	206.08
		318	35.25	42.93			179.31	206.25

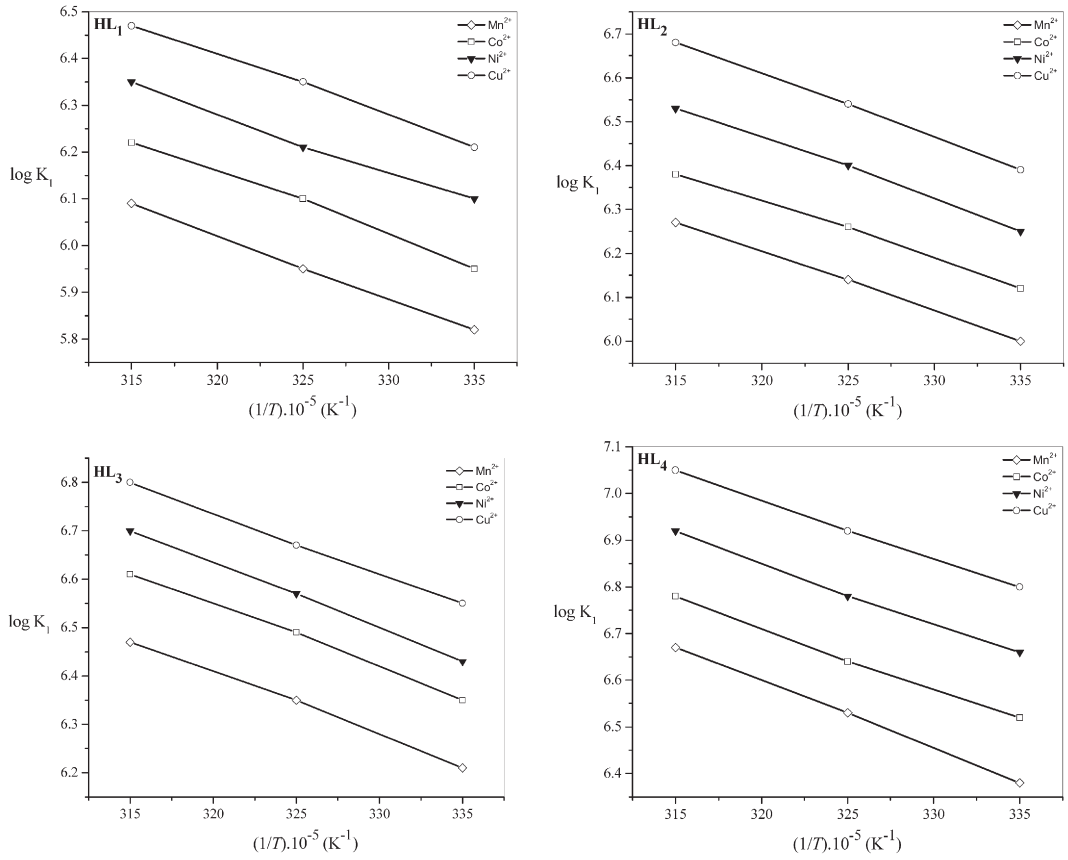

Fig. 7. Van't Hoff plot of log K_1 of M^{n+} complexes with ligands (HL_n) against 1/T.

From the ΔG and ΔH values, one can deduce the entropy ΔS using the well-known relationships (4) and (6):

$$\Delta S = (\Delta H - \Delta G)/T \quad (6)$$

The thermodynamic parameters of the dissociation process of ligands (**HL_n**) are recorded in Table 4. From these results, the following can be made:

(i) The pK^H values decrease with increasing temperature, i.e. the acidity of ligands increases [18].
(ii) Positive values of ΔH indicate that dissociation is accompanied by absorption of heat and the process is endothermic.
(iii) Positive values of ΔG indicate that the dissociation process is not spontaneous [16].
(iv) Negative values of ΔS are due to increased order as a result of the solvation processes.

All the thermodynamic parameters of stepwise stability constants for the complexes of ligands (**HL_n**) are recorded in Table 6. The obtained values ΔH and ΔS can then be considered as the sum of two contributions: (a) Release of H_2O molecules and (b) Metal-ligands bond formation. Examination of these values shows that:

(i) The stability constants (log K_1 and log K_2) for quinoline azo dyes complexes increase with increasing temperature, i.e. its stability constants increase with increasing temperature as shown in Figs. 7 and 8.
(ii) The negative values of ΔG for the complexes formation suggest a spontaneous nature of such process [9].
(iii) The positive values of ΔH mean that the complex formation processes are endothermic and favored at higher temperature.
(iv) The positive values of ΔS are confirming that the complex formation processes are thermodynamically favorable [16].

Inspection of the results in Table 6 reveals that the pK^H values of 5-(4-derivative phenyl azo)-8-hydroxyquinoline and its derivatives are influenced by the inductive or mesomeric effect of the substituents. **HL_1** has a lower acidic character (higher pK^H values) than **HL_2**. This is quite reasonable because the presence of *p*-CH_3 group (i.e. an electron-donating effect) will enhance the electron density by their high positive inductive or mesomeric effect, whereby a stronger O—H bond is formed. The presence of *p*-Cl group (i.e. an electron-withdrawing effect) will lead to the opposite effect [18].

4. Conclusion

5-(4-Derivative phenyl azo)-8-hydroxyquinoline and its derivatives (**HL_n**) have been synthesized and characterized by different spectroscopic techniques. The proton-ligand dissociation constant of ligands (**HL_n**) and metal–ligand stability constants of their complexes with metal ions (Mn^{2+}, Co^{2+}, Ni^{2+} and Cu^{2+}) at different temperatures were determined. The stability constants of the formed complexes increase in the order Mn^{2+}, Co^{2+}, Ni^{2+} and Cu^{2+}. The dissociation process is non-spontaneous, endothermic and entropically unfavorable. The formation of the metal complexes has been found to be spontaneous, endothermic and entropically favorable. The stability constants (log K_1 and log K_2) for the complexes increase with increasing temperature. The pK_1^H value of the ligands increases in the order of **HL_1** > **HL_2** > **HL_3** > **HL_4**.

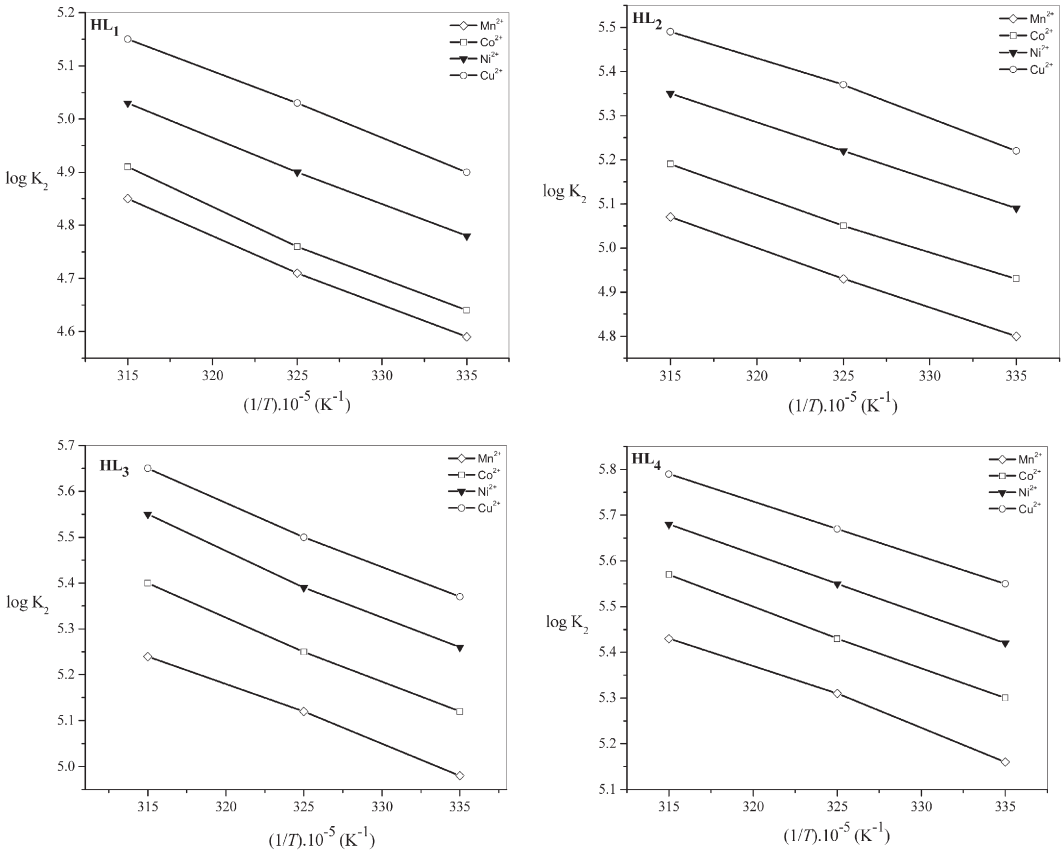

Fig. 8. Van't Hoff plot of log K_2 of M^{n+} complexes with ligands (HL_n) against 1/T.

References

[1] M.A. Diab, A.A. El-Bindary, A.Z. El-Sonbati, O.L. Salem, J. Mol. Struct. 1018 (2012) 176–184.
[2] N.A. El-Ghamaz, E.M. El-Menyawy, M.A. Diab, A.A. El-Bindary, A.Z. El-Sonbati, S.G. Nozha, Solid State Sci. 30 (2014) 44–54.
[3] N.A. El-Ghamaz, M.A. Diab, A.A. El-Bindary, A.Z. El-Sonbati, S.G. Nozha, Spectrochim. Acta A 143 (2015) 200–212.
[4] M.A. Diab, A.Z. El-Sonbati, A.A. El-Bindary, A.M. Barakat, Spectrochim. Acta A 116 (2013) 428–439.
[5] C. Karadaş, D. Kara, J. Food Compos. Anal. 32 (2013) 90–98.
[6] M.A. Diab, A.A. El-Bindary, A.Z. El-Sonbati, O.L. Salem, J. Mol. Struct. 1007 (2012) 11–19.
[7] A. Nezhadali, G. Taslimi, Alex. Eng. J. 52 (2013) 797–800.
[8] A.F. Shoair, A.R. El-Shobaky, E.A. Azab, J. Mol. Liq. 203 (2015) 59–65.
[9] A.A. El-Bindary, A.Z. El-Sonbati, M.A. Diab, A.M. Barakat, J. App. Sol. Chem. Mode. 2 (2013) 191–196.
[10] A.Z. El-Sonbati, G.G. Mohamed, A.A. El-Bindary, W.M.I. Hassan, A.K. Elkholy, J. Mol. Liq. 209 (2015) 625–634.
[11] T. Cheng, Q. Li, Z. Zhou, Y. Wang, S. Bryant, AAPS J. 14 (2012) 133–141.
[12] N.A. El-Ghamaz, A.A. El-Bindary, A.Z. El-Sonbati, N.M. Beshry, J. Mol. Liq. 211 (2015) 628–639.
[13] A.Z. El-Sonbati, A.A. El-Bindary, A.F. Shoair, R.M. Younes, Chem. Pharm. Bull. 49 (2001) 1308–1313.
[14] G.H. Jeffery, J. Bassett, J. Mendham, R.C. Deney, Vogel's Textbook of Quantitative Chemical Analysis, fifth ed. Longman, London, 1989.
[15] A.A. El-Bindary, A.Z. El-Sonbati, M.A. Diab, E.E. El-Katori, H.A. Seyam, Int. J. Adv. Res. 2 (2014) 493–502.
[16] A.A. El-Bindary, A.Z. El-Sonbati, M.A. Diab, Sh.M. Morgan, J. Mol. Liq. 201 (2015) 36–42.
[17] A.Z. El-Sonbati, G.G. Mohamed, A.A. El-Bindary, W.M.I. Hassan, M.A. Diab, Sh.M. Morgan, A.K. Elkholy, J. Mol. Liq. 212 (2015) 487–502.
[18] A.A. El-Bindary, M.A. Hussein, R.A. El-Boz, J. Mol. Liq. 211 (2015) 256–267.
[19] Z. Bikadi, E. Hazai, J. Chem. Inf. 11 (2009) 1–15.
[20] T.A. Halgren, J. Comput. Chem. 17 (1998) 490–519.
[21] G.M. Morris, D.S. Goodsell, J. Comput. Chem. 19 (1998) 1639–1662.
[22] R.J.B. Wets, Mathematics of Operations Research 6 (1981) 19–30.
[23] A.Z. El-Sonbati, M.A. Diab, A.A. El-Bindary, A.M. Eldesoky, Sh.M. Morgan, Spectrochim. Acta A 135 (2015) 774–791.
[24] A.Z. El-Sonbati, M.A. Diab, A.A. El-Bindary, G.G. Mohamed, Sh.M. Morgan, Inorg. Chim. Acta 430 (2015) 96–107.
[25] N.A. El-Ghamaz, A.Z. El-Sonbati, M.A. Diab, A.A. El-Bindary, G.G. Mohamed, Sh.M. Morgan, Spectrochim. Acta A 147 (2015) 200–211.
[26] N.A. El-Ghamaz, A.Z. El-Sonbati, M.A. Diab, A.A. El-Bindary, M.K. Awad, Sh.M. Morgan, Mater. Sci. Semicond. Process. 19 (2014) 150–162.
[27] M.M. Ghoneim, A.Z. El-Sonbati, A.A. El-Bindary, M.A. Diab, L.S. Serag, Spectrochim. Acta A 140 (2015) 111–131.
[28] A.Z. El-Sonbati, A.A. El-Bindary, R.M. Ahmed, J. Sol. Chem. 32 (2003) 617–623.
[29] A.A. El-Bindary, A.F. Shoair, A.Z. El-Sonbati, M.A. Diab, E.E. Abdo, J. Mol. Liq. 212 (2015) 570–584.
[30] L.E. Orgel, An Introduction to Transition Metal Chemistry Ligand Field Theory, Methuen, London, 1966, p. 55.